Computers and Electronics in Agriculture 75 (2011) 64–70

Contents lists available at ScienceDirect

Computers and Electronics in Agriculture

journal homepage: www.elsevier.com/locate/compag

Original paper

Development of a method using multispectral imagery and spatial pattern metrics to quantify stress to wheat fields caused by *Diuraphis noxia*

Georges F. Backoulou[a,*], Norman C. Elliott[b], Kristopher Giles[a], Mpho Phoofolo[a], Vasile Catana[a]

[a] Oklahoma State University, 127 Noble Research Center Stillwater, OK 74078, United States
[b] USDA-ARS 1301N Western Rd. Stillwater, OK 74075, United States

ARTICLE INFO

Article history:
Received 20 January 2010
Received in revised form
20 September 2010
Accepted 22 September 2010

Keywords:
Multispectral image
Plant stress
Remote sensing
Spatial pattern metrics
Diuraphis noxia

ABSTRACT

The Russian wheat aphid, *Diuraphis noxia*, is an important pest of winter wheat, *Triticum aestivum*, and barley, *Hordeum vulgare* that has caused an annual economic loss estimated at over 1 billion dollars since it first appeared in the United States. The objective of this study was to determine the potential of combining multispectral imagery with spatial pattern recognition to identify and spatially differentiate *D. noxia* infestations in wheat fields. Multispectral images were acquired using an MS3100-CIR multispectral camera. *D. noxia*, drought, and agronomic conditions were identified as major causes for stresses found in wheat fields. Seven spatial metrics were computed for each stress factor. The analysis of spatial metrics quantitatively differentiated the three types of stress found within wheat fields. Detection and differentiation of wheat field stress may help in mapping stress and may have implications for site-specific monitoring systems to identify *D. noxia* infestations and help to target pesticide applications.

1. Introduction

The Russian wheat aphid, *Diuraphis noxia* (Mordvilko) (Homoptera: Aphididae), is one of the most important pests of winter wheat, *Triticum aestivum*, and barley, *Hordeum vulgare* (Puterka et al., 2007). In the United States, *D. noxia* was first identified near Muleshoe, TX in 1986 (Morisson and Peairs, 1998). Since then, *D. noxia* spread rapidly, from Texas to the Rocky Mountains and Canada (Thomas et al., 2002). The annual economic loss to the small grain industry in the U.S. caused by *D. noxia* is estimated at over 1 billion dollars (Archer and Bynum, 1992; Morisson and Peairs, 1998; Webster et al., 2000).

D. noxia infests wheat fields from plant emergence to maturity. It induces stress to the wheat crop by damaging plant foliage and disrupting the plant's physiology (Burd and Burton, 1992; Miller et al., 1994). Stress may be defined as disturbance that adversely influences plant growth (Jackson, 1986). *D. noxia* affects plant morphology and physiological change such as a decrease in photosynthesis (Mitternicht, 2003). *D. noxia* feeds on young wheat leaves causing symptoms that include longitudinal chlorotic streaking and leaf rolling, which reduce productivity (Burd et al., 1998; Miller et al., 1994; Webster et al., 1987). Field scouting for aphid infestations can be tedious and time consuming especially when aphid populations are very high (Hodgson et al., 2007). Remote sensing technology may offer an alternative to the traditional ground-based insect count assessment of wheat fields. Remote sensing is the science and art of obtaining information about objects through the analysis of digital data acquired by a device that is not in contact with the object under investigation (Lillesand and Kiefer, 2000). The value of this technology in detecting stress to vegetation has been demonstrated in many systems (Adams et al., 1999; Mitternicht, 2003; Riley, 1989). Remote sensing offers the possibility to identify areas of wheat plant stress within fields more efficiently than traditional sampling approaches. Yang et al. (2004) stated that it is possible to quantitatively describe an aphid infestation using remote sensing.

Several studies have used remote sensing techniques to investigate stress induced by aphids to wheat. Yang et al. (2004) used ground based multispectral radiometry to detect stress induced by the greenbug, *Schizaphis graminum*, on wheat plants. Mirik et al. (2007) characterized the spectral properties of wheat plants infested by *D. noxia* using a ground-based hyperspectral spectrometer. Elliott et al. (2007) used an airborne multispectral remote sensing system to investigate the injury to wheat plants induced by *D. noxia*. Merrill et al. (2009) developed a spatial model using Landsat imagery and field observations based on environmental factors such as topography and soil types to predict densities of *D. noxia*. These studies demonstrated the potential of spectral information for characterizing stress to wheat plants caused by aphids.

* Corresponding author at: OSU Entomology and Plant Pathology, 127 Noble Research Center Stillwater, OK 74078, United States. Tel.: +1 405 624 4141x263.
E-mail addresses: Georges.Backoulou@okstate.edu, backoul@hotmail.com (G.F. Backoulou).

0168-1699/$ – see front matter © 2010 Elsevier B.V. All rights reserved.
doi:10.1016/j.compag.2010.09.011

Although spectral pattern analysis can distinguish plants stressed by aphids from healthy plants, there are difficulties differentiating one type of stress from another. Analysis of spectral patterns in wheat resulting from various causal agents is difficult because the spectral response of wheat plants to stress is similar for stress from many other stress causing agents. For example, Yang (2005) experienced difficulties differentiating stress induced by *S. graminum* from that induced by moisture deficit using spectral reflectance analysis. This difficulty suggested the need for additional spatial information to assist in distinguishing various types of stress to wheat plants in fields.

D. noxia infestations are not uniform in wheat fields, but in fact have a distinctly aggregated spatial distribution that is species specific (Feng and Nowierski, 1992). Spatial pattern analysis has the potential to supplement spectral pattern information to differentiate among stress factors (Mirik et al., 2007). It might be possible to use information about *D. noxia* spatial distribution to augment information derived from multispectral remote sensing to distinguish stress caused by *D. noxia*.

Our objective was to identify whether spatial pattern analysis of multispectral image data could be used to distinguish the stress caused by *D. noxia* infestation in wheat fields from that caused by other common stress factors. We hypothesized that a disruption of the integrity of homogenous areas of healthy wheat plants caused by *D. noxia* and other stress factors could be detected and spatially distinguished using spatial pattern analysis. Furthermore, we surmised that *D. noxia* infestations have specific patterns that can be differentiated from that of other stresses. To test our hypothesis we obtained multispectral images of wheat fields exhibiting stress caused by *D. noxia* infestation and other types of stress. We created thematic maps with two categories, one representing stress and the other healthy wheat, and then conducted analysis of the resulting maps using spatial metrics to determine if we could differentiate areas in wheat fields stressed by *D. noxia* from areas stressed by other causes.

This study is an ongoing project that contains several components. This first component demonstrates the potential of using multispectral image data and spatial pattern information to detect and differentiate the types of stress found in wheat fields. A second component will demonstrate the potential of building a model to discriminate the types of stress and validate the methodology.

2. Materials and methods

2.1. Study area and data acquisition

We conducted the study in commercial wheat fields located near Boise City, Oklahoma, 36°73′N, −102°51′W. The area has a mean annual temperature of 13.05 °C, and mean annual precipitation of 470.6 mm. In this region, wheat is planted from September to October and harvested from June to July the next year.

A field survey was a critical component before acquiring any imagery. The survey consisted of: exploring the region to find wheat fields that were stressed by *D. noxia* and/or other stress factors; measuring and recording geographic locations of each selected wheat field, measuring and recording geographic locations of tarps set at each selected field; and also, measuring and recording geographic locations of stressed areas within fields that presented symptoms of *D. noxia* infestation or other factors.

We define stress as any biotic and abiotic conditions or mixture of them that negatively affected the growth development of wheat plants within fields. Areas of stressed wheat fields were noticeable within fields. They were characterized by mosaics of patches of stunted plants that obviously differed from the surroundings areas of healthy wheat plants.

Two features regarding stress in wheat fields were observed during our ground field survey. First, stress was not uniformly distributed through a field. Some areas within a field were heavily stressed and others showed no evidence of stress. Thus, stress was patchily distributed. Second, three general types of stress were observed. Stress caused by (1) *D. noxia* infestation, (2) drought, and (3) by agronomic conditions. The term “agronomic conditions” was used to include stress related to poor site preparation including tillage, plant germination, or fertilization. Stressed areas (patches) were geographically referenced, as previously described, and the cause of the stress was determined and entered in a computer file along with the geographic coordinates of the approximate center of the particular stressed patch.

Areas of stressed wheat plants caused by *D. noxia* were similar with areas of stressed wheat caused by drought. They were both characterized by stunted wheat plants that exhibited symptoms such as erect, rolled, or curled leaves. The difference between both types of stress was that wheat plants damaged by *D. noxia* appeared purplish. *D. noxia* could be found hiding in leaves that were in tubular form. When unrolling leaves of wheat plants, they presented longitudinal yellowish and whitish streaks.

D. noxia were not present in patches of wheat plants damaged by drought conditions or were present in very low numbers that caused minimal damage to wheat plants in the patch. In these patches, wheat plants appeared yellow or bronze in color. Stressed patches of wheat that were not categorized as damaged by *D. noxia* or by drought were grouped in a single category designated as caused by agronomic conditions. *D. noxia* were not present in these patches or were present in minimal numbers.

Multispectral imagery and field survey data were collected during the months of April and May 2005, and 2007, from eight commercial wheat fields. Multispectral imagery of each wheat field was acquired using an MS3100-CIR, a multispectral camera manufactured by Duncan Tech (Techpark, Singapore). The camera acquires 1392×1040 pixels resolution images in three co-registered channels and uses a color separating prism with three charge coupled device sensors that cover three channels: near infrared, red and green (Channel 1, Channel 2 and Channel 3), centered at 800, 650, and 550 nm with bandwidths of 65, 40, and 40 nm (Hi-Tech Electronics, 2008). The MS3100-CIR camera was mounted nadir, pointing below the fuselage of a Cessna 172 aircraft. This camera used a progressive scan to capture sequential area images that were saved to a computer hard drive in *.tif* format. The width and length of the study area in each field were determined by the field of view of the camera when flown at an approximate altitude of 1500 m above ground. At that altitude, the image width and length were slightly less than 0.8 km.

The process of collecting imagery required first finding fields that were infested by *D. noxia* and/or exhibited other types of stress. Four silver plastic tarps (1.5 m × 1.5 m) were placed along the edge of the fields in a rectangular pattern. The coordinates of the center of each tarp were recorded using a handheld GPS receiver. The locations of the tarps were used by the pilot while imaging to orient the airplane above each selected study field, and also to geometrically correct each image. Each field was surveyed for plant stress caused by *D. noxia* and other factors, such as drought and nutrient deficiency. The geographic coordinate of the approximate center of each contiguous area within a field with stressed wheat plants was measured using a handheld GPS receiver. These field survey data were used to locate and select wheat fields heavily stressed, calibrate remotely sensed imagery, and test the visual accuracy of remote sensing outputs.

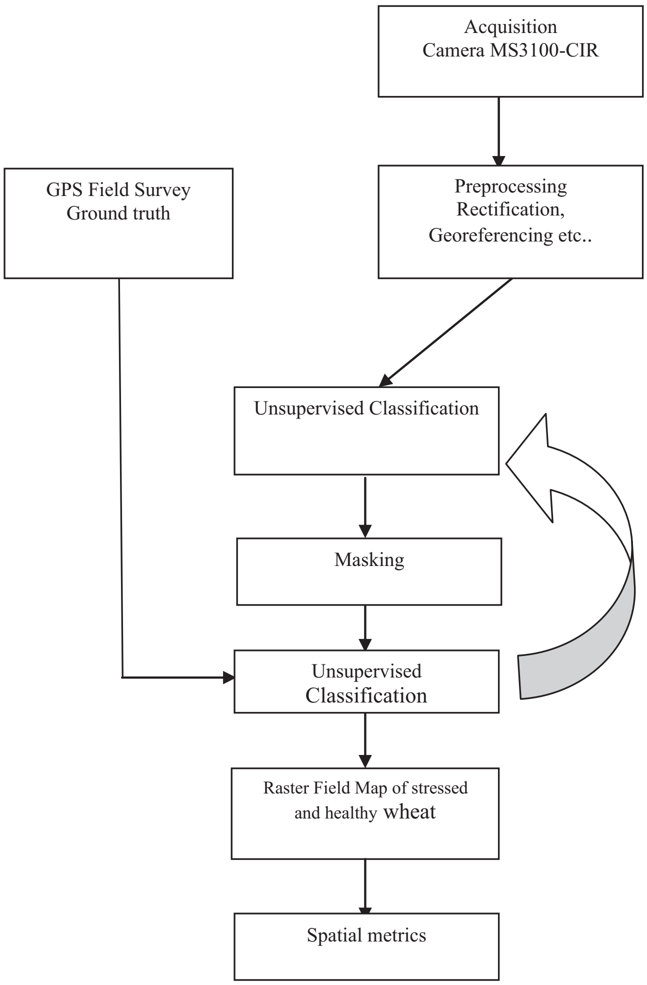

Fig. 1. Flow chart of image analysis.

2.2. Image processing and analysis

ERDAS Imagine software (version 8.6) was used to process and classify multispectral images. The three image channels were used in the image processing. Fig. 1 illustrates the overall image processing method, which involved preprocessing, processing and analyzing images.

During the image preprocessing, image data were geometrically verified and corrected using the ground reference data. After correction, images were registered using the 2003 National Agricultural Imagery Program (NAIP) data available online at the USDA-Farm Service Agency web site. Each image was projected onto a plane and made to conform to a Universal Transverse Mercator (UTM) map projection system using ERDAS Imagine software. We then cut out a subset of each image to focus on areas that were of primary interest. After each image was rectified and subset, the output was then used in image processing.

Mapping the spatial characteristics of stress induced by *D. noxia* and other factors required classifying the subset of multispectral image of each field. In the classification process, pixels of each image were categorized into one of two classes; (1) healthy wheat where wheat plants were not damaged and (2) stressed wheat. The stressed wheat class included areas of wheat plants stressed by *D. noxia*, drought, or agronomic conditions. The healthy wheat class consisted of contiguous areas that were not injured by *D. noxia*, drought or any other problem. The unsupervised classification was used to aggregate the pixels into natural spectral groupings in each image (ERDAS, 1999). Twenty classes were originally selected with an approximate true color technique. Pixels reflecting areas of healthy wheat plants were masked to separate areas of healthy wheat plants from areas of stressed wheat plants. The image masking procedure was repeated iteratively until all areas within an image were classified as either healthy or stressed.

The post classification process included a GIS filtering using neighborhood analysis that was based on the majority of pixels in a given class to clean up pixels that were not correctly classified. A layer of GPS ground-truth points collected during the field survey was used to verify the accurate location points for each stressed wheat patch. The product of the classification process was a raster thematic map with two classes, healthy wheat, and stressed wheat (damaged by *D. noxia* infestation, drought, or agronomic conditions) (Fig. 2).

2.3. Quantifying stress

Healthy wheat patches were not our point of focus; therefore, healthy wheat patches were excluded from the analysis. FRAGSTATS software (version 3.3), a public domain computer program developed by McGarigal and Marks (1995), was used to quantify the spatial pattern of stressed wheat patches. FRAGSTATS software computes spatial metrics at each of three levels: patch, class, and landscape, are three ecological terms used extensively in the implementation and description of FRAGSTATS (Raines, 2002). We defined a patch as a contiguous area of stressed or not stressed wheat plants that differed from its matrix. A class was the grouping of all patches of the same type. The grouping of all classes formed the landscape, which in this study is the entire wheat field. Thus, FRAGSTATS software computes spatial statistics at three levels (patch, class, and field) to describe the spatial characteristics of each. We considered patches of any size, as grain, and as the smallest sampling unit for this study. Therefore spatial pattern metrics calculated at the patch level were appropriate (Botequilha Leitao et al., 2006; Turner et al., 1989, 2001). We generated a set of seven spatial pattern metrics from classified multispectral subset images of each wheat field.

A large number of spatial metrics can be computed from a thematic map (Turner et al., 2001). These metrics can be grouped into general categories that describe the size and distribution of patches of each stress factor; the complexity of the shape of patches; and spatial metrics that describe the proximity of the patches of each type of stress. Spatial pattern metrics we selected are described in Table 1. These metrics were selected for their ability to illustrate characteristics such as size, geometric shape, and proximity of stressed patches to one-another. These spatial metrics were computed from subset images of eight wheat fields that exhibited stress caused by *D. noxia*, drought, and a variety of agronomic conditions.

The patch area metric (AREA), as its name indicates, measures the size of a patch of wheat area that could be either stressed or not. It characterizes the composition of the wheat field. Perimeter metric (PERIM) measures the length of the perimeter of each patch. It is also a metric related to the size of the patch and to its shape. In general, the larger the size of the patch, the greater the perimeter length. However, for patches of equal area, the more complex the shape of patch the greater the perimeter length (McGarigal and Marks, 1995).

Radius of Gyration (GYRATE) is a metric that measures the average distance between the center of a patch and the outmost extent of its contiguous cells (Botequilha Leitao et al., 2006). GYRATE has been interpreted as a measure of the average distance an organism can move across a field while the organism remains within a focal patch (Keitt et al., 1997). This metric estimates the level of connectivity of patches of each type of stress (Botequilha Leitao et al., 2006; Gustafson and Parker, 1992). According to Botequilha

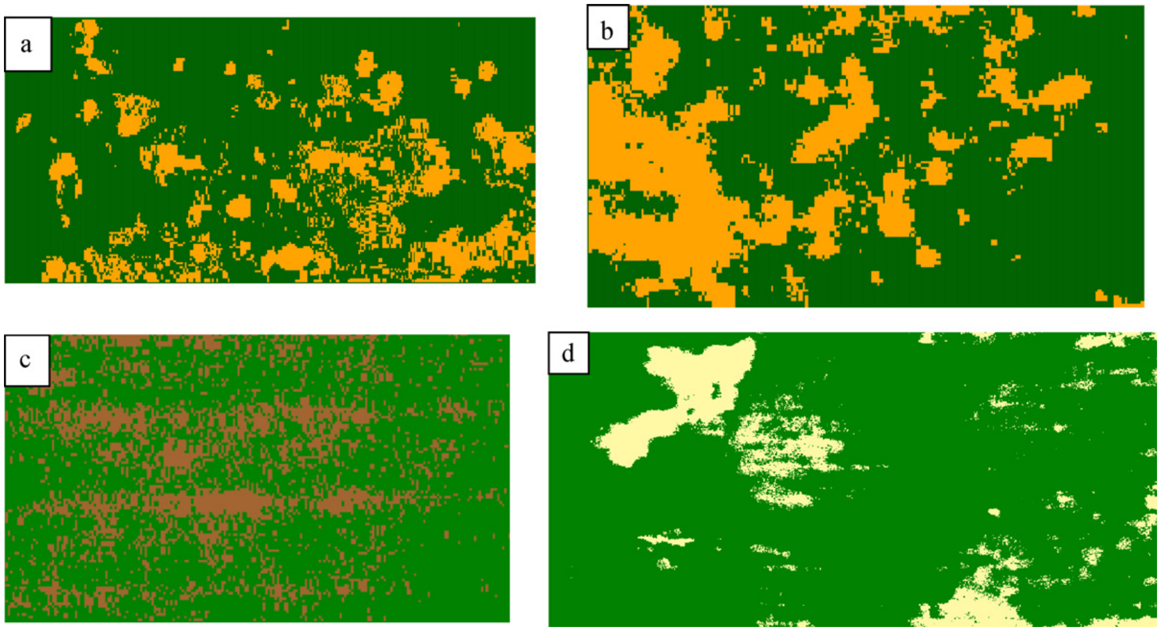

Fig. 2. Classified images of wheat fields showing the predominant types of stress: (a) and (b) *D. noxia*, (c) agronomic conditions, and (d) drought. Color green represents areas of healthy wheat plants. (For interpretation of the references to color in this figure legend, the reader is referred to the web version of the article.)

Leitao et al. (2006), the larger the patch the greater the GYRATE, and higher values of GYRATE are found in elongated patch shapes.

SHAPE and fractal dimension are unitless spatial metrics that measure the geometric complexity of patches. Both spatial metrics are computed from the relationship between the perimeter length and the area of the patch. SHAPE index is a ratio of the patch perimeter to the perimeter of the theoretically most compact patch (McGarigal et al., 2002). It measures the geometric complexity of a patch, and deals with the spatial arrangement of patches within wheat field (Botequilha Leitao et al., 2006). SHAPE is a comparative metric that can be used effectively to compare patches complexity within and between different fields (Botequilha Leitao et al., 2006). The minimum value of shape index is 1 when patches are maximally compact. Patches with that value are more likely to be squared or almost square. The value of shape index increases without limit as patch shape becomes more irregular (McGarigal et al., 2002).

Fractal dimension index (FRAC) is another metric that measures the shape complexity. It is a descriptor of the spatial pattern that can be used to compare changes through time that may occur in particular field, and patches of different sizes. Fractal dimension index equals twice the logarithm of patch perimeter over the logarithm of the patch area (McGarigal et al., 2002). The value of the fractal dimension index ranges between 1 and 2. It approaches 1 for patches that are likely to be squared or almost squared, and it approaches 2 for patches tending to be circular. The fractal dimension index also measures the degree of shape complexity of patches.

The proximity index (PROX) and the Euclidean Nearest Neighbor Distance index (ENN) are both configuration metrics that refer to the tendency for patches to be relatively distant or isolated in space, from other patches of the same or similar type of stress (McGarigal et al., 2002). PROX is unitless and deals with the spatial arrangement of patches. It is computed as a ratio of the sum of patch areas over the nearest distance squared between the patch and the focal patch of similar type whose edges are within a specific distance of the focal patch (McGarigal and Marks, 1995). PROX value ranges upwards from zero with no limit. Larger values of PROX indicate neighboring patches of the same type of stress are larger and closer together, indicating that patches are less isolated; otherwise smaller values of PROX indicate that patches are apart from each other and are more likely to be smaller in area (Botequilha Leitao et al., 2006; McGarigal et al., 2002). This spatial metric considers the size and proximity distance of all patches that have edges within a 50-m radius, the distance chosen for this analysis. PROX quantifies the spatial distribution of a specific patch type across the wheat field. The metric is an interpretive value that is much more used in comparative analysis between different patches or comparing

Table 1
Description and definition of spatial metrics computed from classified images using FRAGSTATS.

	Spatial metrics	Abbreviations	Description
Size	Patch area	AREA	The measure of the size (m^2) of each patch within a wheat field
	Patch perimeter	PERIM	Total distance around each patch (m)
	Radius of Gyration	GYRATE	The measure of patch extent, involves the mean distance (m) between each cell in the patch and the patch centroid
Shape	Shape index	SHAPE	The ratio of patch perimeter to the minimum perimeter for the maximally compact patch of the same patch area across the class
	Fractal dimension index	FRAC	The ratio of 2 times logarithm of patch perimeter to logarithm of patch area
Proximity	Proximity index	PROX	The ratio of the sum of patch areas to the nearest edge-to-edge distance squared between patches in a specific radius
	Euclidean Nearest Neighbor Distance	ENN	The measure of the shortest straight-line distance between the focal patch and its nearest neighbor of the same class

(Description adapted from McGarigal and Marks, 1995).

Table 2
The field configuration metrics at patch level, computed from wheat field classified images using FRAGSTATS software. The table contains the means and standard error of spatial metrics by aspect of configuration and types of stress.

Field configuration	Spatial metrics	*D. noxia*		Drought		Agronomic conditions	
		Mean	SE	Mean	SE	Mean	SE
Size	PATCH AREA (m^2)	7.30	1.11	17.00	1.95	3.14	0.81
	PERIM (m)	16.30	1.96	26.57	2.41	7.84	0.95
	GYRATE (m)	1.43	0.10	2.61	0.23	0.51	0.03
Shape	SHAPE (unitless)	1.39	0.02	1.45	0.03	1.19	0.02
	FRAC (unitless)	1.12	0.04	1.57	0.06	0.87	0.05
Isolation\proximity	PROX (unitless)	78.96	5.06	38.93	2.40	27.64	2.62
	ENN (m)	1.79	0.03	1.17	0.01	1.37	0.03

Table 3
ANOVA of wheat stress. The table compares the variance of field spatial metrics of each types of stress. The *P*-values (<0.0001) indicate that at least one of the three types of stress is statistically different.

Field configuration	Spatial metrics	R^2	Sum squares	Mean squares	*F* value	*F*-value
Size	PATCH AREA (m^2)	0.01	171166.1	85583.1	25.7	<0.0001
	PERIM (m)	0.01	295182.9	147591.4	24.5	<0.0001
	GYRATE (m)	0.02	3720.5	1860.2	48.8	<0.0001
Shape	SHAPE (unitless)	0.014	61.6	30. 8	36.0	<0.0001
	FRAC (unitless)	0.02	428.8	214.4	47.7	<0.0001
Isolation\proximity	PROX (unitless)	0.023	2329064.2	1164532.1	57.8	<0.0001
	ENN (m)	0.073	331.0	165.5	196.2	<0.0001

spatial configuration of patches in different landscapes (Botequilha Leitao et al., 2006; McGarigal et al., 2002).

The ENN measures the shortest distance from one patch to another patch of the same type (McGarigal and Marks, 1995). It measures the field configuration and measures the spatial distribution of patches in a particular field. Its value ranges upwards from zero with no limit. This range may be important in management practices, as we consider that a wheat field is a landscape that has been fragmented by *D. noxia* infestation. The range is the shortest distance that must be crossed in order to find another patch of the same type. This information may help to assess the dispersion of the infestation in a given distance to allow the application of a pesticide or other type of management practice. More detailed information about metrics can be found in McGarigal et al. (2002).

Statistical analyses were conducted using SAS software version 9.1 (SAS Institute, Inc., Cary, 2002). We performed PROC GLM (general linear model) with the Fisher‘s Least Significant Different (LSD) test to compare spatial metrics computed for the three types of stress (*D. noxia*, drought and agronomic conditions) (SAS Institute Inc., 1990).

3. Results and discussion

Three common types of overriding stress were identified within eight wheat fields. These types of stress consisted of stress caused by *D. noxia*, drought conditions, and problems that resulted presumably from stress caused by improper field preparation or planting, such as non-uniform germination along the planting line or yellowed plants due to non-uniform fertilizer distribution.

The results of classification of multispectral image data are illustrated in Fig. 2. These results were achieved based on the simultaneous utilization of the three bands that comprise each image. The results show patches of the three types of stress in their matrices that represent areas of healthy wheat plants in each field. Fig. 2a and b displays patches of wheat field that were caused by *D. noxia*. Their spatial pattern in the classified image visually differs from the other types of stress. Areas of *D. noxia* infestation have a particular spatial configuration that looks like patches forming a constellation, grouped in close proximity to one another. Areas of a wheat field damaged by drought conditions are displayed in Fig. 2d. They consisted of several large patches of damaged wheat plants. Wheat field areas exhibiting damage due to cultural practices tend to be somewhat linear in appearance, arranged along the planting lines in the field (Fig. 2c).

A total of 4943 stressed wheat patches were derived from the eight classified images. These comprised 1582 wheat patches caused by *D. noxia*, 1749 by drought, and 1612 by agronomic conditions. The set of seven patch-based spatial pattern metrics computed were used to quantify the specific spatial configuration (spatial character and arrangement) of stressed patches contained

Table 4
The results of Fisher's LSD test comparing pairwise means of metric and their 95% confidence interval (in parenthesis) by type of stress. The difference between each type of stress was statistically different. However, there was no difference between patches of wheat damaged by drought and patches damaged by *D. noxia* when comparing values of SHAPE metric.

Stress comparison	Differences between means and 95% confidence						
	PATCH AREA (m^2)	PERIM (m)	GYRATE (m)	SHAPE	FRAC	PROX	ENN (m)
Drought – *D. noxia*	9.70 (5.77 to 13.60)	9.84 (4.60 to 15.10)	1.17 (0.76 to 1.60)	0.06 (−0.01 to 0.12)*	0.45 (0.30 to 0.60)	−40.04 (−49.70 to −30.40)	−0.62 (−068 to −0.56)
Drought to agronomic conditions	13.86 (9.9 to 17.70)	18.73 (13.50 to 23.99)	2.10 (1.70 to 2.50)	0.26 (0.20 to 0.32)	0.70 (0.56 to 0.84)	11.30 (1.70 to 20.90)	−0.21 (−0.27 to −0.56)
D. noxia to agronomic conditions	4.20 (0.15 to 8.20)	8.90 (3.50 to 14.30)	0.92 (0.49 to 1.34)	0.20 (0.14 to 0.26)	0.26 (0.10 to 0.40)	51.33 (41.48 to 61.20)	0.41 (0.35 to 0.47)

within each wheat fields. The means and standard errors of the seven spatial pattern metrics for each type of stress are displayed in Table 2. Examination of the table reveals that patches of wheat plants caused by *D. noxia* have greater mean values of spatial metrics such as PROX and ENN than patches caused by drought and agronomic conditions. Patches of wheat caused by drought conditions have greater mean values of AREA, PERIM, GYRATE, SHAPE, and FRAC metrics than patches caused by *D. noxia*, or agronomic conditions. Patches damaged by agronomic conditions have lower mean values of all seven spatial pattern metrics than patches damaged by *D. noxia* or drought conditions.

Table 3 illustrates the analysis of variance (ANOVA) that compares the mean of spatial pattern metrics among the three types of stress. The *P*-value of each spatial pattern metric comparison reveals that each metric differs significantly among at least one of the three types of stress at 0.5 significant level. Table 4 reports the Fisher's LSD pairwise comparisons of means of each type of stress and 95% confidence limits. The pairwise comparison of spatial metrics by type of stress using the LSD test, showed that all spatial metrics were statistically different for the three types of stress except for the SHAPE metric, which did not exhibit statistical significance difference between stressed patches caused by *D. noxia* and drought (Table 4).

The visual assessment of each patch and the analysis of each spatial pattern metrics have illustrated a difference among the types of stress that damage wheat fields. This difference suggests that it is possible to use the spatial features or characteristics of each patch to distinguish the three types of stress found in wheat fields. These spatial features of each patch are based on the size, shape, and proximity or isolation of each type of stress.

Patches of healthy or damaged wheat plants were spatially arranged in the mosaic pattern within wheat fields. The set of spatial metrics selected for this study helped in quantifying the spatial pattern characteristics of each type of stress. Patches of wheat damaged by the three types of stress had distinctly different shapes and spatial arrangements. These differences could possibly be used to differentiate fields where *D. noxia* is the primary stress factor from fields where other stress factors predominate.

According to the analysis of the spatial pattern metrics, patches of wheat caused by *D. noxia* were smaller than patches of wheat caused by drought conditions and larger than patches of wheat caused by agronomic conditions. They were circular and close to one another appearing in constellation format pattern. Patches of wheat damaged by drought conditions had higher shape complexity. These patches were larger than patches of wheat caused by *D. noxia* and agronomic conditions. They were elongated and less connected. Patches of wheat caused by agronomic conditions were smaller than the two to other types of stress. They were less complex, in linear aspect, and were apart from each other.

Detecting and quantifying wheat field stress may help in mapping *D. noxia* infestations and may have implications for site-specific monitoring systems for *D. noxia* and developing pesticide application recommendations. The findings of this study will allow for more practical methods to detect *D. noxia* infested wheat fields using multispectral imagery. Ultimately, the goal is to provide growers and managers with an immediately available, non-destructive, inexpensive method to detect *D. noxia* infestations, and the ability to apply site-specific pest control practices when and where needed.

4. Conclusion

Findings presented and discussed above indicate that:

(1) It is possible to use multispectral images acquired with the Duncan MS3100-CIR camera mounted on the fuselage of an aircraft to detect stress within wheat fields caused by a number of factors.
(2) It is possible to differentiate among stress causing factors by augmenting the multispectral imagery by spatial pattern analysis.
(3) Patches of wheat stressed by *D. noxia*, drought, and agronomic conditions differed spatially with respect to size, shape, and spatial arrangement within a wheat field.

Acknowledgements

The authors thank Drs. Robert Hunger and Justin Talley for reviewing this manuscript. This work was approved for publication by the Director of the Oklahoma Agricultural Experiment Station, and supported in part of the Oklahoma Agricultural Experiment Station Project OKLO2334. The authors acknowledge the great help and assistance provided by Mr. Tim Johnson of USDA-ARS, Stillwater, OK.

References

Adams, M.L., Philpot, W.D., Norvell, W.A., 1999. Yellowness index: an application of spectral second derivatives to estimate chlorosis of leaves in stressed vegetation. International Journal of Remote Sensing 20 (18), 3663–3675.
Archer, T.L., Bynum Jr., E.D., 1992. Economic injury level for the Russian wheat aphid on dryland winter wheat. Journal of Economic Entomology 85, 987–992.
Botequilha Leitao, A., Miller, J., Ahern, J., McGarigal, K., 2006. Measuring Landscapes: A Planner's Handbook. Island Press, Washington, DC.
Burd, J.D., Burton, G.W., 1992. Total chlorophyll fluorescence profiles of Russian wheat aphid resistant and susceptible wheat. In: Proceedings of the Fifth Russian Wheat Aphid Conference, Great Plains Agriculture Council Publications 142, Fort Worth, TX, pp. 101–108.
Burd, J.D., Butts, R.A., Elliott, N.C., Shufran, K.A., 1998. Seasonal development, overwintering biology, and host plant of Russian wheat aphid (Homoptera: Aphididae) in North America. In: Response Model for an Introduced Pest—The Russian Wheat Aphid. Thomas Say Publications in Entomology, Lanham, MD, pp. 65–99.
Elliott, N.C., Mirik, M., Yang, Z., Dvorak, T., Rao, M., Micheis, J., Walker, T., Catana, V., Phoofolo, M., Giles, K., Royer, T., 2007. Airborne multi-spectral remote sensing of Russian wheat aphid injury to wheat. Southwestern Entomologist 2 (4), 213–219.
ERDAS, 1999. ERDAS Field Guide, fifth ed. ERDAS, Inc., Atlanta, GA.
Feng, M.G., Nowierski, R.M., 1992. Spatial distribution and sampling plans for four species of cereal aphids (Homoptera: Aphididae) infesting spring wheat in southwestern Idaho. Journal of Economic Entomology 85, 830–837.
Gustafson, E.J., Parker, G.R., 1992. Relationships between landcover proportion and indices of landscape spatial pattern. Landscape Ecology 7 (2), 101–110.
Hi-Tech Electronics, 2008. Ducan Tech MS3100 Camera, RGB (3-CCD), Color IR Camera-AreaScan/Line Scan camera. Available from: http://www.hitech.com.sg/rl/multispectral/MS3100_Data_Page.htm. Visited March 03, 2008.
Hodgson, E.W., McCornack, B.P., Koch, K.A., Ragsdale, D.W., Johnson, K.D., O'Neal, M.E., Cullen, E.M., Kraiss, H.J., DiFonzo, C.D., Behnken, L.M., 2007. Field validation of speed scouting for soybean aphid. Crop Management, doi:10.1094/CM-2007-0511-01-RS.
Jackson, R.D., 1986. Remote sensing of biotic and abiotic plant stress. Annual Reviews of Phytopathology 24, 265–287.
Keitt, T.H., Urban, D.L., Milne, B.T., 1997. Detecting critical scales in fragmented landscapes. Conservation Ecology [online] 1 (1), 4, Available from: http://www.consecol.org/vol1/iss1/art4/. Visited October 04, 2009.
Lillesand, T.M., Kiefer, R.W., 2000. Remote Sensing and Image Interpretation, fourth ed. John Willey and Sons, New York, NY.
McGarigal, K., Marks, B.J., 1995. FRAGSTATS: Spatial Pattern Analysis Program for Quantifying Landscape Structure. USDA For. Serv. Gen. Tech. Rep. PNW-351.
McGarigal, K., Cushman, S.A., Neel, M.C., Ene, E., 2002. FRAGSTATS: Spatial Pattern Analysis Program for Categorical Maps. Available from: http://www.umass.edu/landeco/research/fragstats/fragstats.html. Visited November 25, 2007.
Mitternicht, G., 2003. Vegetation indices derived from high-resolution airborne videography for precision crop management. International Journal of Remote Sensing 24 (14), 2855–2877.
Miller, H., Porter, D.R., Burd, J.B., Mornhinweg, D.W., Burton, R.L., 1994. Physiology effects of Russian wheat aphid (Homoptera: Aphididae) on resistant and susceptible barley. Journal of Economic Entomology 87, 493–499.
Mirik, M., Michels Jr., G.J., Kassymzhanova-Mirik, S., Elliott, N.C., 2007. Reflectance characteristics of Russian wheat aphid (Hemiptera: Aphididae) stress and

abundance in winter wheat. Computers and Electronics in Agriculture 57 (2), 123–134.
Merrill, S.C., Holtzer, T.O., Peairs, F.B., Lester, P., 2009. Modeling spatial variation of Russian wheat aphid overwintering population densities in Colorado winter wheat. Journal of Economic Entomology 102 (2), 533–541.
Morisson, W.P., Peairs, F.B., 1998. Response model concept and economic impact. In: Response Model for an Introduced Pest—The Russian Wheat Aphid. Thomas Say Publications in Entomology, Lanham, MD, pp. 1–11.
Puterka, G.J., Burd, J.D., Porter, D., Shufran, K., Baker, C., 2007. Distribution and diversity of Russian wheat aphid (Hemiptera: Aphididae) biotypes in North America. Journal of Economic Entomology 100 (5), 1679–1684.
Raines, G.L., 2002. Description and comparison of geologic maps with FRAGSTATS: a spatial statistic program. Computer and Geosciences 28, 169–177.
Riley, J.R., 1989. Remote sensing in entomology. Annual Review of Entomology 34, 247–271.
SAS Institute Inc., 1990. SAS/STAT® User's Guide, Version 6, fourth ed., vol. 1. SAS Institute Inc., Cary, NC, 943 pp.
Thomas, J., Hein, G., Baltensperger, D., Nelson, L., Haley, S., 2002. Managing the Russian Wheat Aphid with resistant varieties. File NF307 under: Insect and Pests. C-5, Field Crops. Nebraska Cooperative Extension. University of Nebraska, Lincoln, NE.
Turner, M.G., O'Neill, R.V., Gardner, R.H., Milne, B.T., 1989. Effects of changing spatial scale on the analysis of landscape pattern. Landscape Ecology 3 (3/4), 153–162.
Turner, M.G., Gardner, R.H., O'Neill, R.V., 2001. Landscape Ecology in Theory and Practice: Pattern and Process. Springer-Verlag, New York.
Webster, J.A., Starks, K.J., Burton, R.L., 1987. Plant resistance studies with *Diuraphis noxia* (Homoptera: Aphididae), a new United States wheat pest. Journal of Economic Entomology 80, 944–949.
Webster, J., Treat, R., Morgan, L., Elliott, N.C., 2000. Economic Impacts of the Russian Wheat Aphid and Greenbug in the Western United States 1993–1994, 1994–1995, and 1997–1998. U.S. Department of Agriculture, ARS Service Report PSWCRL Rep. 00-001.
Yang, Z., Rao, M.N., Elliott, N.C., Kindler, S.D., Popham, T.W., 2004. Using ground-based multispectral radiometry to detect stress in wheat caused by greenbug (Homoptera: Aphididae) infestation. Computers and Electronics in Agriculture 47, 121–135.
Yang, Z., 2005. Detection of greenbug infestation on wheat using ground-base radiometry. Doctorate Thesis. Oklahoma State University, Stillwater, OK.